

Journal Pre-proof

Polyaniline-metal oxide-nano-composite as a nano-electronics, opto-electronics, heat resistance and anticorrosive material

Harish Kumar, Anurag Boora, Ankita Yadav, Rajni, Rahul



PII: S2211-7156(20)30024-2

DOI: <https://doi.org/10.1016/j.rechem.2020.100046>

Reference: RECHEM 100046

To appear in: *Results in Chemistry*

Received date: 19 February 2020

Accepted date: 24 April 2020

Please cite this article as: H. Kumar, A. Boora, A. Yadav, et al., Polyaniline-metal oxide-nano-composite as a nano-electronics, opto-electronics, heat resistance and anticorrosive material, *Results in Chemistry* (2020), <https://doi.org/10.1016/j.rechem.2020.100046>

This is a PDF file of an article that has undergone enhancements after acceptance, such as the addition of a cover page and metadata, and formatting for readability, but it is not yet the definitive version of record. This version will undergo additional copyediting, typesetting and review before it is published in its final form, but we are providing this version to give early visibility of the article. Please note that, during the production process, errors may be discovered which could affect the content, and all legal disclaimers that apply to the journal pertain.

© 2020 Published by Elsevier.

Polyaniline-Metal oxide-nano-composite as a nano-electronics, opto-electronics, heat resistance and anticorrosive material

Harish Kumar¹, Anurag Boora¹, Ankita Yadav¹, Rajni¹ & Rahul¹

1. Dept. of Chemistry, School of Chemical Sciences, Central University of Haryana, Mahendergarh -123031 (India)

* Author for correspondence: harishkumar@cuh.ac.in, <https://orcid.org/0000-0002-8559-2302>

Abstract:

Nanoparticles when combined with conducting polymer polyaniline leads to increase in advanced functional properties. Cu, Ni and Zn metal oxide (CNZMO) nanoparticles were synthesized by Sol-gel technique. Conducting polymer polyaniline was synthesized by low temperature chemical synthesis method. *In situ* technique was used to synthesize CNZMO-Polyaniline (PANI) nanocomposite. Metal nanoparticles, polyaniline and metal oxide-polyaniline nano-composite were characterized by UV-visible, FTIR, FESEM, XRD and TGA/DTA techniques. Opto-electronic, thermal and anticorrosive properties of CNZMO-PANI nano-composite was compared with their bulk counterpart. The optical band gap of the PANI-nano-composite was found to be 1.72 eV which is lesser than pure polyaniline (3.2 eV) and bulk counterpart (2.2 to 3.6 eV). Anticorrosive property of CNZMO-PANI nano-composite was tested for mild steel in 0.1 N hydrochloric acid medium and was found to be good corrosion inhibitor at 80 ppm concentration. CNZMO-PANI nanocomposite was found to be thermally stable up to 650 °C. Hence, synthesized CNZMO-PANI nano-composite has large number of applications in the field of nano-electronics, heat resistance composite material, optoelectronics and as anticorrosive material.

Keywords: Metal nanoparticles, Nano-composite, Sol-Gel method, Polyaniline, Conducting polymer.

1. Introduction:

Manipulation of material at nanoscale for creating distinctive substrates with vast capacity to change society is referred to as nanotechnology [1,2]. Implementation and acceptance of nanotechnology is very vast and rapid in the field of education, training and research and development [3]. Materials and products made from Nanotechnology may have a very enormous range of applications, as in heat resistance material, nanoelectronics, optoelectronics, biomaterials energy production, consumer products, anticorrosive materials etc.

Conducting polymers are the organic polymers which conduct electricity, commonly known as synthetic metals [4]. Conducting polymers have improved properties over metals such as strength, elasticity, plasticity, toughness, light weight, greater workability and economy [5]. Conducting polymers also have very low resistivity of around 10^{-14} cm^{-1} [5-7]. Polyphenylene, Polyacetylene, Polypyrrole, Polyaniline, Polythiophene, etc. are some examples of conducting polymers. Table 1 shows the list of few commonly used conducting polymers [8]. Polyaniline is a significant conducting polymer and has become popular over the past few years [9-12]. The conjugated - electron system existing in PANI increases its conductivity in a favorable way which then unlocks the path to achieve its several uses like battery electrode material, transparent conductor, biosensors, corrosion protection practices, etc. [13].

Manawwer Alam and his group [14] calculated the electrical and optical data of PANI/ZnO nanocomposite. Red shift was observed by the addition of ZnO nanoparticles. The nanocomposite was thermally stable upto $120 \text{ }^\circ\text{C}$ and displayed $3.0 \times 10^{-2} \text{ Scm}^{-1}$ conductivity. Raju and his group [15] synthesized Nickel–Zinc ferrite/polymer nano-composite by mechanical ball milling process and used XRD, SEM and FT-IR spectroscopy techniques for characterization. They reported that the permittivity and permeability value decreases on increasing content of polymer.

In this paper, we have synthesized Cu, Ni and Zn metal oxide nanoparticles by sol-gel techniques. Conducting polymer polyaniline was synthesized by low temperature chemical oxidative

technique. Characterization of nanoparticles and conducting polymer polyaniline was carried out by UV-visible, FTIR, FESEM, XRD and TGA/DTA techniques. CNZMO-PANI nano-composite was synthesized by *in-situ* method. Optical, thermal and anticorrosive study of CNZMO-PANI nano-composite was carried out.

2. Material and Methods:

2.1. Sol gel synthesis of nanoparticles:

All the chemicals used i.e. $\text{CuCl}_2 \cdot 2\text{H}_2\text{O}$, NiCl_2 , ZnCl_2 , AlCl_3 , aniline, oxalic acid, ethanol, HCl were of analytical reagent (AR) grade and solutions were prepared using double distilled water (JSGW, Ambala 427/3). AlCl_3 was procured from Fisher Scientific having percentage purity 98.7 %, Ethanol was procured from CSS analytical reagent having percentage purity of 99.9%, Aniline was procured from Rankem having percentage purity 99.0%, Oxalic acid was procured from Finar having percentage purity 99.5%, ZnCl_2 was procured from Rankem having percentage purity 98.9%, $\text{CuCl}_2 \cdot 2\text{H}_2\text{O}$ was procured from CDH having percentage purity 99.0% and NiCl_2 was procured from Sigma-Aldrich having percentage purity 99.99 %.

The 0.5 M metal salt solution was prepared ($\text{CuCl}_2 \cdot 2\text{H}_2\text{O}$, NiCl_2 and ZnCl_2). A turbid solution was obtained. Then few drops of concentrated nitric acid (HNO_3) were added to adjust the solution pH to 1-2. This solution was labeled as A. Standard oxalic acid and pure ethanol was mixed in the ratio of 1:4. This solution was termed as B. Solution B was added to solution A in a drop wise manner at a constant temperature of 70.0 °C with continuous stirring at 600 RPM (IKA C-MAG). The reaction was continued to 6.0 hours. A green color slurry was obtained. Then the slurry was kept in an oven maintained at a constant temperature of 100.0 °C for 24.0 hours. After drying, washing of product was carried out with water and then acetone. The product was again dried for 6.0 hours at 70.0 °C. The metal oxide nanoparticles were characterized by UV-visible spectroscopy (UV -2600 Shimadzu), FTIR (Bruker Model No. 12498665), XRD, FESEM, and TGA/DTA (Shimadzu Coop. Model No. 545) techniques.

2.2 Oxidative polymerization low temperature synthesis of conducting polymer PANI nano-composite:

The 1.0 M aniline solution + 1.0 M HCl solution and 1.0 M metal nanoparticles solution (CuO, ZnO and NiO) were taken in a borosil beaker. The beaker was kept in ice to maintain low temperature ~ 4.0 °C. Then 1.0 M AlCl₃ solution was taken in a burette and added to the beaker containing metal oxide and aniline solution in drop wise manner with constant stirring (at 600 rpm). The solution was kept undisturbed for 7.0 hours. The product was filtered by using SS vacuum filtration. The mother liquor obtained was centrifuged and the product obtained was washed with water, dilute hydrochloric acid and then with organic solvent (ethanol). The product was then dried for 24.0 hours in an oven maintained at a constant temperature of 70.0 °C. The green-black solid obtained was crushed into fine powder using mortar-pestle and then was stored in a glass vial bottle.

3 Results and discussion:

3.1 FTIR spectra of nanoparticles and CNZMO-PANI nano-composite

The prepared nanocomposite was examined through FTIR spectroscopy via assigning the functional groups to impurity if present and to confirm the purity of metal oxide nanoparticles. Figure 2 shows FTIR spectra of metal nanoparticles and PANI-nanocomposite. It is apparent from FTIR spectra that peaks positioned at 520.5, 692.35 and 821 cm⁻¹ are due to CuO, ZnO and NiO metal oxide nanoparticles and broad peak at 3381 cm⁻¹ is due to OH stretching vibrations present due to atmospheric moisture content in sample. The FTIR spectrum (Figure 2) shows bands of PANI-nano-composite at 3383, 1625.75, 1488, 1358, 1295.85, 826.24, 822.75, 692.69 and 515.4 cm⁻¹. The peak at 3383, 1625.75, 1488 and 1358 cm⁻¹ occurs because of quinonoid and benzenoid ring bending and stretching vibrations. The peak at 1358 cm⁻¹ features to C-N stretching vibration adjacent to quinonoid ring. Absorption peak at 1295.85 cm⁻¹ resembles to C-N stretching vibrations of secondary aromatic amine. Peak at 1488 cm⁻¹ is because of C=C stretching and peak

at 826.24 cm^{-1} is because of C-H bending. These peaks confirmed the formation of polyaniline. The presence of peaks at 821.75 , 692.19 and 525.4 cm^{-1} are due to CuO, ZnO and NiO metal oxide nanoparticles in PANI-nano-composite spectra confirms the *in-situ* mechanism of PANI-nano-composite formation. Peaks at $450\text{-}550\text{ cm}^{-1}$ corresponds to ZnO nanoparticles [16].

3.2 Optical Characterization

3.2.1 UV-Visible absorption study

The HOMO and LUMO are separated through energy gap called band gap which is of vital importance as energy gap governs conductivity and optical absorption property of PANI-nano-composite. The optical performance of PANI-nano-composite is based on collection of several PANI chains and electronic combination of pi-system. Transition of charge transporters are examined by UV-visible spectrum. Figure 3 shows UV-visible absorption spectra of metal nanoparticles and PANI-nano-composite. The maximum absorbance at 206.50 nm (λ_1) wavelength was found to be 1.046 for nanoparticles and at 245.50 nm (λ_2) as 0.6125 for CNZMO-PANI nano-composite. A bathochromic shift was observed for maximum absorbance when we switch from metal nanoparticles to PANI-metal oxide nanocomposite. This red shift is due to interaction between metal oxide nanoparticles and PANI nanocomposite rings which significantly increase the extent of electron delocalization. The peak at 245.50 nm is because of $\Pi\text{-}\Pi^*$ transitions which is related to degree of conjugation between the neighboring phenylene rings in polymeric chain. The decrease in absorbance maximum from 1.046 to 0.6125 proves that CNZMO-PANI nanocomposite are spongy in nature and small expansion in volume takes place during *in-situ* synthesis of CNZMOO-PANI nanocomposite which is due to entrapment of metal oxide nanoparticles in the cavity of benzene ring of PANI.

3.2.2 Optical band gap analysis

Band gap of CNZMO-PANI-nano-composite was measured by absorbance coefficient data as function of wavelength using Tauc relation given as under [17]:

$$\alpha h\nu = B(h\nu - E_g)^n \quad \dots(1)$$

Where, α = absorption coefficient, $h\nu$ = photon energy, B = band gap tailing parameter, E_g = characteristic band gap energy and n = transition probability index.

The value of absorption coefficient, α , at corresponding wavelengths is calculated using Lambert's-Beer relation [18].

$$\alpha = 2.303A/t \quad \dots(2)$$

Where, t is the thickness of cuvette (path length) which is 10 mm and A is the absorbance coefficient. $h\nu$ is calculated by the use of relation given as under:

$$h\nu = 1242 \alpha/\lambda \quad \dots(3)$$

Plot of $(\alpha h\nu)^2$ versus $h\nu$ is linear function of indirect allowed transitions in PANI-nano-composite and are shown in Figure 4. The optical energy gap of CNZMO-PANI-nano-composite is 1.72 eV, which is because of π - π^* transition from valence to conduction band whereas the pure PANI value is reported as 3.2 eV [19]. A decrease in optical band gap was observed (3.2 to 1.72 eV) after the addition of nanoparticles to polyaniline. Hence, the conductivity of CNZMO-PANI nano-composite is enhanced.

3.3 XRD Analysis

Crystallinity of conducting polymers is a matter of interest due to their highly ordered systems exhibiting high conductivity. Thus to examine crystallinity of PANI-nano-composite and metal salt nanoparticles, they are exposed to XRD analysis and results are showed in Figures 5. Peaks in X-ray diffraction pattern of metal oxide nanoparticles are indexed at 18° (111), 23° (200) and 30° (211). Peaks in X-ray diffraction pattern of CNZMO-PANI nanocomposite are indexed at 19° (110), 23° (111) and 30° (211). The peak indexed at 20.2° corresponds to definite separation between rings of polymeric chains [20]. On comparing X-ray diffraction pattern of metal oxide nanoparticles with CNZMO-PANI nanocomposite, it is observed that peaks become sharper and degree of crystallinity increases in case CNZMO-PANI nanocomposite. The intensity of peak

indexed at 19° (110) also increases. The sharp high intensity peaks indicates that the CNZMO-PANI nano-composite formed is crystalline in nature. The peak indexed at 30.0 and 40.0° corresponds to hexagonal wurtzite zinc oxide with high order of crystallinity (JCPDS card no. 36-1451 space group P63mc).

With the help of Scherer equation [21], average particle size of the nanoparticles was calculated

$$\text{as:} \quad d = k \lambda / \beta \cos \theta \quad \dots(4)$$

Where, d = average particle size of ordered crystalline domains which may be smaller or equal to the grain size, k = dimensionless shape factor with a value close to unity (≈ 0.9), λ = X-ray wavelength, β = line broadening at half the maximum intensity, θ = Bragg angle. From the above equation, the average particle size (d) of particles was observed to be 40-60 nm.

3.4 Thermogravimetric Analysis

The Figure 6 shows TGA/DTA curve of CNZMO-PANI nano-composite when exposed to constant heating rate of $5.0^{\circ}\text{C}/\text{min}$. The green coloured thermo-gravimetric curve represents the TGA and blue coloured thermo-gravimetric curve represents DTA. As observed from TGA curve (Figure 6) that the first major weight loss takes place at 180.0°C is due to loss of moisture and other adsorbed gases and the second major weight loss takes place at 550.0°C is due to loss of one or two metal oxide nanoparticles and carbon dioxide gas from the nano-composite. The gradual and steady weight loss over the broad temperature range represents high order of thermal stability of CNZMO-PANI nanocomposite. CNZMO-PANI nano-composite was found to be thermally stable up to 670.0°C . Hence, CNZMO-PANI nanocomposite can be used as heat resistance material.

3.5 FESEM analysis

Figure 7 shows FESEM images of metal nanoparticles and CNZMO-PANI nano-composite, respectively. Average particle size of metal nanoparticles was found to be 50 to 80 nm. It is

observed from Figure 7 that metal oxide nanoparticles are uniformly distributed in conducting polymer PANI matrix. Metal oxide nanoparticles get entrapped in benzene ring cavity leading to small expansion in PANI nano-composite making it some spongy like material. Few metal oxide nanoparticles were also present between junctions of APNI chain network. A phase contrast picture is not appeared due to complete superposition of metal oxide nanoparticles by the PANI ring framework. But a detailed study reveals that bright phase represent metal oxide nanoparticles and somewhat dark region corresponds to PANI ring framework.

4. Anti-corrosive study of CNZMO-PANI nano-composite:

Mild steel sheet was procured from local market of Mahendergarh (Haryana) and cut into eight small coupons of size $3.0 \times 1.5 \text{ cm}^2$ with metal sheet cutter. All the metal sheet coupons were mechanically polished using different grades of emery papers numbered as 100, 200, 300 and 600 μ , respectively in order to have mirror like finish. The mild steel coupons were washed initially with water and then acetone and then dried with hot air blower. Weights (initial weight) of the mild steel coupons were recorded. 0.1 g of PANI-nano-composite was added in 100 mL of 0.1 N HCl solution. This solution was termed as stock solution. From the stock solution different concentration of PANI nano-composite as corrosion inhibitors were prepared.

Then mild steel coupons were dipped in the above prepared solutions (each beaker contains one mild steel coupon) for 3.0 hours with and without PANI-nano-composite and the beakers were covered with aluminium foil and left undisturbed. After 3.0 hours, the mild steel coupons were taken out and washed with water and then with acetone and then dried. Weight (final weight) of each mild steel coupons were recorded. From the weight loss of sample, corrosion rate and percentage corrosion inhibition efficiency was calculated by using ASTM standards [22-24]. Table 2 shows initial and final weights, weight loss, corrosion rate and percentage corrosion inhibition efficiency (PCIE) of CNZMO-PANI nanocomposite at different concentration (20 to 100 ppm) at room temperature. It is observed from Table 2 that weight loss decreases and

corrosion rate decreases and percentage corrosion inhibition efficiency increases with increase in concentration of CNZMO-PANI nanocomposite. More than 91 % protection to mild steel was provided by CNZMO-PANI nanocomposite at 100 ppm when exposed to 0.1 N HCl solutions as corroding medium at room temperature. Hence, CNZMO-PANI nanocomposite proves to be very good anticorrosive composite material for providing protection to mild steel.

5. Conclusions:

CNZMO-PANI nano-composite was synthesized by *in-situ* method. IR data affirms uniform mixing of $\text{CuCl}_2 \cdot 2\text{H}_2\text{O}$, $\text{NiCl}_2 \cdot 6\text{H}_2\text{O}$ and ZnCl_2 in PANI matrix. Thermogravimetric study reveals that the synthesized CNZMO-PANI nano-composite is thermally stable up to 670 °C. Through XRD analysis, the crystalline nature of the synthesized PANI-nano-composite was confirmed. Synthesized CNZMO-PANI nano-composite acts as very good corrosion inhibitor for mild steel in 0.1 N HCl solution as corroding medium at 80 and 100 ppm concentration. Optical band gap of CNZMO-PANI nanocomposite was found to be less than pure metal nanoparticles and PANI. Synthesized CNZMO-PANI nano-composite was tested as nano-electronics, heat resistance composite material, optoelectronics and anticorrosive material to protect the metals and their alloys from corrosion.

Conflict of Interest:

There is no conflict of interest with anybody or any agency in publishing this research article.

Acknowledgments:

We are very thankful to the CUH authorities for providing all types of infrastructural support and laboratory facility for carrying out this research work.

References:

- [1] Mama El R, Sanaa M, Miloud E, Fatima E S, Larbi O, Khalid L. Recent progress in nanocomposites based on conducting polymer: Applications as electrochemical sensors. *Internat. Nano Letters*. 2018; 8: 79-99.
- [2] Ehsani A, Bigdeloo M, Assefi F, Kiamehr M, Alizadeh R, Ternary nanocomposite of Conductive polymer/chitosan biopolymer/metal organic framework: Synthesis, characterization and electrochemical performance as effective electrode materials in pseudocapacitors, *Inorganic Chemistry Communications*. 2020; 115: 107885. doi.org/10.1016/j.inoche.2020.107885
- [3] Yasser Z, Kyong Y R, Analysis of the Connecting Effectiveness of the Interphase Zone on the Tensile Properties of Carbon Nanotubes (CNT) Reinforced Nanocomposite. *Polymers*. 2020; 12: 896. doi:10.3390/polym12040896.
- [4] Ma CCM, Chen YJ, Kuan HC. Polystyrene nanocomposite materials—preparation, mechanical, electrical and thermal properties, and morphology. *J Appl Polym Sci* 2006; 100(1); 508-15. <https://doi.org/10.1002/app.23221>
- [5] Zhao Y, Qi X, Ma J, Song L, Yang Y, Yang Q. Interface of polyimide-silica grafted with different silane coupling agents: molecular dynamic simulation. *J Appl Polym Sci* 2018; 135(4): 45725. doi.org/10.1002/app.45725
- [6] Ghaemy M, Qasemi S, Ghassemi K, Bazzar M. Nanostructured composites of poly(triazole-amide-imide) and reactive titanium oxide by epoxide functionalization: thermal, mechanical, photophysical and metal ions adsorption properties. *J Polym Res* 2013; 20 (10). doi.org/10.1007/s10965-013-0278-2
- [7] Robertson CG, Lin CJ, Rackaitis M, Roland CM. Influence of particle size and polymer/filler coupling on viscoelastic glass transition of particle-reinforced polymers. *Macromolecules* 2008; 41: 2727-31. <https://doi.org/10.1021/ma7022364>
- [8] Li C, Benicewicz BC, Synthesis of well-defined polymer brushes grafted onto silica nanoparticles via surface reversible addition/fragmentation chain transfer polymerization, *Macromolecules*, 2005, vol. 38, pp. 5929-36. <https://doi.org/10.1021/ma050216r>
- [9] Bartholome C, Beyou E, Bourgeat EL, Chaumont P, Zydowicz N. Nitroxide-mediated polymerizations from silica nanoparticle surfaces: “graft from” polymerization of styrene using a triethoxysilylterminated alkoxyamine initiator. *Macromolecules* 2003; 36: 7946-52. DOI: 10.1021/ma034491u
- [10] Giri PK, Bhattacharyya S, Singh DK, Kesavamoorthy R, Panigrahi BK, Nair KGM. Correlation between microstructure and optical properties of ZnO nanoparticles synthesized by ball milling. *J Appl Phys* 2007; 102(9): 093515. doi.org/10.1063/1.2804012
- [11] Sharma S, Pande SS, Swaminathan P. Top-down synthesis of zinc oxide based inks for inkjet printing. *RSC Adv* 2017; 7(63): 39411-19. doi.org/10.1039/C7RA07150G
- [12] Priyadarshana G, Kottegoda N, Senaratne A, DeAlwis A, Karunaratne V. Synthesis of magnetite nanoparticles by top-down approach from a high purity ore. *J Nanomater* 2015; 1-8. doi.org/10.1155/2015/317312
- [13] Chen JS, Zhu T, Yang XH, Yang HG, Lou XW. Top-down fabrication of r-Fe₂O₃ single-crystal nanodiscs and microparticles with tunable porosity for largely improved lithium storage properties. *J Am Chem Soc*. 2010; 132(38): 3162-4. doi.org/10.1021/ja1060438
- [14] Salah N, Habib SS, Khan ZH, Memic A, Azam A, Alarfaj E. High-energy ball milling technique for ZnO nanoparticles as antibacterial material. *Int J Nanomed*. 2011; 6: 863-9. DOI: 10.2147/IJN.S18267
- [15] Cunningham A, Bürgi T. Bottom-up organisation of metallic nanoparticles, In: Rockstuhl, C., Scharf, T., editors, *Amorphous nanophotonics*, Berlin, Heidelberg, Springer; 2013, pp. 1-37.

- [16] Sivakumar K, Kumar SV, Shim JJ, Haldorai Y. Conducting Copolymer/ZnO Nanocomposite: Synthesis, Characterization, and Its Photocatalytic Activity for the Removal of Pollutants, Synthesis and Reactivity in Inorganic, Metal-Organic, and Nano-Metal Chemistry. 2014; 44: 1414–1420. doi.org/10.1080/15533174.2013.809743
- [17] Mott NF, and Davies EA. Electronic Processes in Non-Crystalline Materials. Oxford: Clarendon Press, 1979, 2nd Edn.
- [18] Kumar H, Rani R. Structural and optical characterization of ZnO nanoparticles synthesized by microemulsion route. Int Letters of Chem Phys & Astronomy 2013; 14: 26-36. doi.org/10.18052/www.scipress.com/ILCPA.19.26
- [19] Bouarissa A, Gueddim A, Bouarissa N, Djellali S. Band Structure and optical properties of polyaniline polymer material. Polymer Bulletin 2017; 75: 3023-3033. doi.org/10.1007/s00289-017-2189-6
- [20] Zhang J, Shan D, Mu SJ. Polym Sci Part A–Polym Chem 2008; 45: 5573. <https://doi.org/10.1002/pola.22303>
- [21] Langford J I, Wilson AJC. Scherrer after sixty years: A survey and some new results in the determination of crystallite size. J Appl Crystallogr 1978; 11: 102-113. doi.org/10.1107/S0021889878012844
- [22] Dorcheh A S, Durham R N, Galetz MC. Corrosion behavior of stainless and low-chromium steels and IN625 in molten nitrate salts at 600 °C. Sol Energy Mater Sol Cells 2016; 144: 109-116. doi.org/10.1016/j.solmat.2015.08.011
- [23] Deyab MA. Adsorption and inhibition effect of Ascorbyl palmitate on corrosion of carbon steel in ethanol blended gasoline containing water as a contaminant. Corr Sci 2014; 80: 359-365. doi.org/10.1016/j.corsci.2013.11.056
- [24] Afia L, Salghi R, Bammou L, Bazzi E, Hammouti B, Bazzi L, Bouyanzer A. Anti-corrosive properties of Argan oil on C38 steel in molar HCl solution. J Saudi Chem Soc. 2014; 18: 19-25. doi.org/10.1016/j.jsocs.2011.05.008
- [25] Kosari A, Moayed MH, Davoodi A, Pervizi R, Momeni M, Eshghi H, Moradi H, Corro. Sci. 2014; 78: 138–150.
- [26] Kumar H, Yadav V. *Aloe vera L.* as Green Corrosion Inhibitor for Mild Steel in 5.0 M Hydrochloric Acid Solution. Asian J. of Chem. 2018; 30(3): 474-478. DOI:10.14233/ajchem.2018.20852

Figure captions:

Figure 1. Different steps involved in the synthesis of metal oxide nanoparticles by Sol-gel method.

Figure 2. FTIR spectra of metal oxide nanoparticles and CNZMO-PANI nano-composite.

Figure 3. UV-visible absorption spectra of metal oxide nanoparticles and CNZMO-PANI nano-composite.

Figure 4. Optical band gap observed from Tauc relation in case of CNZMO-PANI nano-composite.

Figure 5. X-ray diffraction pattern of metal oxide nanoparticles and CNZMO-PANI nano-composite.

Figure 6. TGA and DTA curve of CNZMO-PANI nano-composite.

Figure 7. FESEM images of metal oxide nanoparticles and CNZMO-PANI nanocomposites.

Table 1. Structure, optical band gap and DC electrical conductivity of few common conducting polymers.

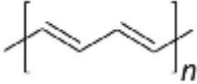
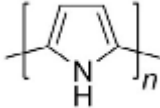
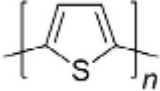
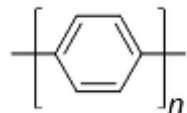
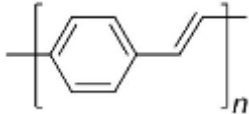
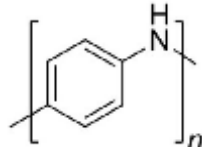
Polymer (the year in which discovered)	Structure	Energy gap (eV)	DC electrical conductivity (S/cm)
Polyacetylene		1.5	$10^3 - 1.7 \times 10^5$
Polypyrrole (1979)		3.1	$10^2 - 7.5 \times 10^3$
Polythiophene (1981)		2.0	$10 - 10^3$
Polyphenylene (1979)		3.0	$10^2 - 10^3$
Poly(p-phenylene vinylene) (1979)		2.5	$3 - 5 \times 10^3$
Polyaniline (1980)		3.2	30-200

Table 2. Weight loss (g), corrosion rate (mils/year) and percentage corrosion inhibition efficiency (PCIE) of blank and CNZMO-PANI nano-composite at different concentrations (20 to 100 ppm) for mild steel in 0.1 N HCl solution at room temperature.

Concentration (ppm)	Initial weight (g)	Final weight (g)	Weight loss (g)	Corrosion rate (mils/yr)	PCIE	PCIE (Lit.)
20	1.2185	1.0833	0.1352	2252.81	42.14	
40	1.2817	1.1477	0.1340	2236.12	42.57	
60	1.2393	1.1642	0.0751	1251.56	67.85	
80	1.2416	1.2025	0.0391	650.81	83.28	88.90 [25]
100	1.2286	1.2092	0.0194	317.06	91.85	51.78 [26]
Blank 1	1.2409	1.0025	0.2384	3971.62	-	
Blank 2	1.2623	1.0314	0.2309	3838.12	-	
Blank 3	1.2348	1.0024	0.2324	3871.5	-	

Average corrosion rate of blanks = 3893.7 mils/yr.

Highlights

- CNZMO-PANI nano-composite was synthesized by *in-situ* method.
- IR data confirms uniform mixing of $\text{CuCl}_2 \cdot 2\text{H}_2\text{O}$, $\text{NiCl}_2 \cdot 6\text{H}_2\text{O}$ and ZnCl_2 in PANI matrix.
- Thermogravimetric study confirms thermally stable up to 670 °C.
- XRD analysis confirms the crystalline nature of PANI-nano-composite.
- CNZMO-PANI nano-composite acts as very good corrosion inhibitor for mild steel.
- CNZMO-PANI nano-composite was investigated as nano-electronics, heat resistance composite material, optoelectronics and anticorrosive material.

Journal Pre-proof